Toxicology Research

Accepted Manuscript

ROYAL SOCIETY OF CHEMISTRY

www.rsc.org/toxicology

Salvianolic acid B protects against doxorubicin-induced cardiac dysfunction via inhibition of er-stress-mediated cardiomyocyte apoptosis

Rongchang Chen, PhD,[a] Guibo Sun, PhD,[ac]* Longpo Yang, PhD,[b] Jian Wang, PhD,[b] Xiaobo Sun, PhD,[ac]*

[a] Institute of Medicinal Plant Development, Chinese Academy of Medical Science, Peking Union Medical College, No 151, North Road Malianwa, Haidian District, Beijing 100094, China

[b] Harbin University of Commerce, Xuehai Street, Songbei District, Harbin, Heilongjiang 150028, China

[c]Zhongguancun Open Laboratory of the Research and Development of Natural Medicine and Health Products

*Correspondence authors. Address: Institute of Medicinal Plant Development, Chinese Academy of Medical Sciences & Peking Union Medical College, No. 151, Malianwa North Road, Haidian District, Beijing 100193, PR China. Tel: +86-010-57833013; Fax: +86-010-57833013. sunxiaoboyzs@163.com (Xiao-bo Sun).

Abstract

Salvia miltiorrhiza Bunge is a well-known medicinal plant in China. Salvianolic acid B (Sal B) is the most abundant bioactive compound extracted from the root of Salvia miltiorrhiza Bunge. The present study investigates the effect of Sal B on cardiac function and cardiomyocyte apoptosis in DOX-treated mice. After pretreatment with Sal B (2 mg/kg i.v.) for 7 d, male BALB/c mice were injected with a single dose of DOX (20 mg/kg i.p.). The cardioprotective effect of Sal B was observed in 7th day after DOX treatment. DOX caused retarded body growth, apoptotic damage, and Bcl-2 expression disturbance. In contrast, Sal B pretreatment (2 mg/kg i.v. before DOX administration) attenuated the DOX-induced apoptotic damage in heart tissues. Futher study indicated that Sal B protected against DOX-induced cardiotoxicity, at least, partially, by inhibiting ER stress, and by being involved in an PI3K/AKT pathway. These findings elucidated the potential of Sal B as a promising reagent for treating DOX-induced cardiotoxicity.

Keywords: Doxorubicin, Salvianolic acid B, Cardiac dysfunction, Endoplasmic reticulum stress, Phosphatidylinositol 3-kinase /protein kinase B.

Introduction

Doxorubicin (DOX) is an anthracycline derivative widely used to treat various cancers. However, the clinical use of DOX may cause hepatotoxicity [1], nephrotoxicity [2], and cardiotoxicity [3], which severely limit its clinical application. The most dangerous side effect of DOX is cardiotoxicity. Lots of studies are looking for measures to attenuated DOX-induced heart injury [4]. The mechanisms for DOX-induced cardiotoxicity are multifactorial, including the increase in oxidant production, altered calcium handling and mitochondrial injury [5, 6]. It has been accepted that DOX-induced ROS generation and oxidative stress play an important function in triggering cardiomyocyte apoptosis [7-10]. Antioxidants reportedly exert protective effects on DOX-induced cardiotoxicity in animal models [11]. Besides, DOX-induced intrinsic activation of the endoplasmic reticulum (ER) stress also serves an important function in myocardial dysfunction [12, 13].

ER is responsible for protein translocation, folding and post-translational modifications [14]. ER stress occurs when ER homeostasis and function are disrupted. Excessive ER stress may ultimately trigger the unfolded protein response (UPR). UPR activation depresses the translational process, then reduces the synthesis of new proteins and activates transcriptional of genes for chaperones and folding enzymes to remove misfolded proteins in ER [15]. However, excessive and prolonged activation of the UPR results in cell apoptosis [16]. Three main ER stress sensors, PKR-like ER kinase (PERK), inositol requiring enzyme 1 (IRE1), and activating transcription factor-6 (ATF-6), will be activated in response to ER stress and then trigger the caspase cascade and ultimately induce apoptosis. Phosphatidylinositol 3-kinase (PI3K)/protein kinase B (Akt) signaling pathway is important in cell growth, survival and proliferation [17]. Akt activation can reduce ER stress-induced cell death and apoptosis [18-20].

Salvia miltiorrhiza Bunge (SM), also known as Danshen in China, has been widely used in clinic in China, Japan, and Korea [21]. The roots of SM have been used for the treatment of various diseases, including coronary heart disease [22], cerebrovascular disease [23], Alzheimer's disease [24], Parkinson's disease [25], renal deficiency [26], hepatocirrhosis [27], cancer [28], and bone loss [29]. Recent studies found that the principal bioactive components of SM are diterpenoid quinines and hydrophilic phenolic acids [30]. Salvianolic acid B (SalB) is the major water-soluble component

extracted from SM. Sal B has strong cardiovascular protective effects by promoting cell survival, inhibiting apoptosis and preserving normal cellular functions [31-33]. Our group also found that Sal B could reduce arsenic trioxide-induced cardiotoxicity and ischemia/reperfusion injury on isolated heart of rats [34, 35]. There is still no documentation for the amelioration of Sal B against DOX-induced cardiotoxicity in mice to date. We observed for the first time, to the best of our knowledge, that Sal B significantly attenuated DOX-induced cardiac dysfunction in mice. The mechanisms may involve the inhibition of ER stress and activation of PI3K/Akt signaling pathway.

Materials and methods

Materials

Sal B standard was purchased from the Shanghai Winherb Medical S & T Development (Shanghai, China, purity > 99%). All antibodies were purchased from Santa Cruz Biotechnology (Santa Cruz, CA, USA). All chemicals were purchased from Sigma (St. Louis, MO, USA).

Animals and experimental protocols

Male BALB/c mice (6-8 weeks old) used in our study were obtained from Vital River Laboratory Animal Technology (Beijing, China). The mice were maintained under standard environmental conditions (room temperature at 25 ± 1℃ and humidity of 60% with 12 h light/dark cycle). The mice were randomly divided into the following groups: (1) Control group: Mice in this group were injected intravenous (i.v.) with normal saline (solvent for DOX and Sal B); (2) Sal B group: Mice in this group were treated with Sal B at a dose of 2 mg/kg i.v. every day for one week; (3) DOX group: Mice in this group were treated with a single dose of DOX at 20 mg/kg i.p.. The dosage of DOX was based on previous reports [36]; (4) Sal B + DOX group: Mice in this group were treated with Sal B at a dose of 2 mg/kg i.v. every day for one week followed by DOX at 20 mg/kg i.p..

Mice were euthanized 7 days after the DOX administration for morphological and cellular studies. The body weights were measured. Echocardiographic measurements and electrocardiography were conducted. Mice were sacrificed and serum was collected for analysis of the enzymatic

activity of LDH, CK and AST by corresponding kit. All mice used in this study were handled in compliance with the guideline for the care and use of laboratory animals established by the Chinese Council on Animal Care.

Echocardiographic measurements

AUBM system (Vevo 770, VisualSonics, Toronto, Canada) equipped with a 7.5 MHz imaging transducer was used for all the examinations. After treatment, the mice were anaesthetized, and the chests were shaved. The mice were placed in recumbent position. Left ventricle internal diameter in systolic phase (LVIDs), left ventricular internal diameter at diastolic phase (LVIDd), fractional shortening (FS) and ejection fraction (EF) were digitally measured on M-mode tracing. In a separate experiment, the mice were injected with a selective PI3K antagonist wortmannin (WM; 1 mg/kg body weight) 1 h before DOX administration (n = 15/group). PI3K inhibitor doses were selected on the basis of previous studies [37, 38].

Electrocardiography (ECG)

ECG recording was taken after the treatment in conscious animals. After treatment with DOX for 7 days, mice were anesthetized with pentobarbital (60 mg/kg, i.p.), and electrodes were inserted in the right hind limb, right front limb, and left hind limb. Data were collected and the heart rate was calculated using 16-Channel Advanced Research Workstation (MP150, BIOPAC Systems, Inc., CA, USA).

Measurement the activity of LDH, CK and AST

Blood samples were obtained from the inner canthus using a capillary tube. The samples were centrifuged at 3000×g for 15 min within 1 h after collection. The activities of lactate dehydrogenase (LDH), creatine kinase (CK), and aspartate transaminase (AST) in the plasma were measured with the corresponding detection kit according to the manufacturers' instruction (Nanjing Jiancheng Bioengineering, China).

Histological studies

Heart tissues were excised and fixed with a 4% solution of formalin in PBS. Following dehydration, the ventricular tissue was embedded in paraffin and was serially cut to produce 4 μm thick sections, which were stained with haematoxylin and eosin and then examined under a light microscope (CKX41, 170 Olympus, Tokyo, Japan) by a pathologist blinded to the groups under study.

Electron microscopy

After treatment, heart tissues of the mice were isolated. The left ventricle was cut into 1 cubic millimeter size and was immersion fixed in phosphate-buffered 2.5% glutaraldehyde (pH 7.4) immediately. Ultrathin sections were fixed with 1% osmium tetroxide, dehydrated through a graded ethanol series, embedded in Epon medium, stained with uranyl acetate and lead citrate and observed under H-7600 electron microscope (HITACHI Medical Corp, Tokyo, Japan).

TUNEL staining

Cardiomyocyte apoptosis was detected using terminal deoxynucleotidyl transferase-mediated dUTP nick end-labelling (TUNEL) assay. This method was performed according to the manufacturer's protocol. After dewaxing and rehydration, the heart sections were incubated with proteinase K for 15 min at room temperature. After rinsing with PBS, the slices were incubated with working-strength terminal deoxynucleotidyl transferase enzyme for 1 h at 37 °C in a humidified chamber, rinsed in a stop/wash buffer and incubated with working-strength anti-digoxigenin conjugate for 30 min at room temperature. After staining with 4′6-diamidino-2-phenylindole, the slices were observed under a fluorescence microscope (Leica, Heidelberg, Germany).

Western blot analysis

Heart tissues were added with saline at a ratio of 1:9 (mg/mL) to form a homogenate. After centrifugation at 7000 rpm for 5 min, precipitation was lysed on ice with tissue protein extraction reagent containing 0.1 mM dithiothreitol and proteinase inhibitor cocktail. The protein concentration was determined using a BCA kit (Pierce Corporation, Rockford, USA). Equal

amounts of protein fractions were separated by 12% SDS-PAGE and were then transferred onto nitrocellulose membranes (Millipore Corporation, USA) in tris-glycine buffer at 100 V for 55 min. The membranes were blocked with 5% (w/v) non-fat milk powder in tris-buffer that containing 0.05% (v/v) Tween-20 (TBST) for 2 h at room temperature. After overnight incubation with appropriate primary antibodies at 4 °C, the membranes were washed thrice with TBST, incubated with secondary antibodies for 2 h at room temperature and then washed again thrice with TBST. Protein blots were developed using an enhanced chemiluminescence solution. Protein expression levels were visualised with Image Lab Software (Bio-Rad, USA).

Statistical analysis

Results from at least three independent experiments were expressed as mean ± SE. Statistical comparisons between different groups were measured using Student's *t*-test or ANOVA with Prism 5.00 software. Statistical significance was considered at $p < 0.05$.

Results

Pretreatment with Sal B attenuated DOX-induced body weight reduction and heart dysfunction in mice

The body and heart weights of mice in the DOX group were lower than those in the control group. Sal B pretreatment caused a recovery of body and heart weights (Fig. 1B and 1C). The relative heart weight index (heart weight to body weight ratio) was similar among all four groups after (Fig. 1D). DOX administration significantly decreased the cardiac function in mice as evidenced by reducing EF and FS and increasing LVIDd and LVIDs compared with saline-treated mice (Fig. 2B). All these pathological changes were attenuated by pre-treatment with Sal B. However, Sal B alone had no influence on body weight and heart function on mice compared with the control group (Figs. 1-2).

Pretreatment with Sal B prevented against DOX-induced heart demage

DOX significantly increased the serum levels of LDH, CK and AST in mice, which indicated a severe cardiac injury. Pretreatment with Sal B inhibited these elevations (Fig. 3A). In the DOX group, the arrangement of cardiac fibres was disrupted, nuclear loss existed in some cardiomyocytes and the intercellular border was obscure (Fig. 3B). Using transmission electron microscopy, clear heart tissue abnormities, such as cytoplasmic vacuolisation, myofibrillar loss, mitochondrial oedema, chromatin condensation and cardiomyocyte necrosis, were observed in DOX-treated mice (Fig. 3C). Pre-treatment with Sal B partially prevented DOX-induced structural abnormalities of heart tissues in mice. Besides, Sal B pretreatment significantly increased DOX-induced reduction of heart rate (Figs. 3D and 3E).

Pretreatment with Sal B inhibited DOX-induced apoptosis and regulated apoptosis-related protein expression in the myocardium

TUNEL assay was performed to investigate the effects of Sal B on cardiomyocyte apoptosis. Few TUNEL-positive cells were detected in the control group, while TUNEL-positive cells increased dramatically in DOX group (2.43% ± 0.51% and 23.05% ± 0.77%, respectively). Pretreatment with Sal B significantly decreased the amount of TUNEL-positive cardiomyocytes (Fig. 4A). The levels of cleaved cas-3 and cas-12 increased significantly in DOX group but were neutralized by Sal B pretreatment (Fig. 4B). Bcl-2/Bax ratio was down-regulated in the mice injected with DOX, which was up-regulated by pretreatment with Sal B (Fig. 4C).

Pretreatment with Sal B attenuated DOX-induced ER stress and regulated ER-related apoptotic protein expression

To explore the potential mechanism responsible for Sal B-offered protection against DOX-induced myocardial damage, protein levels of ER stress markers, GRP78 and CHOP, were evaluated. DOX significantly increased the expression of GRP78 and CHOP. Pretreatment with Sal B effectively ameliorated these changes (Fig. 5A). We next evaluated the expression levels of ER-related apoptotic proteins. DOX treatment significantly up-regulated protein levels of p-IRE-1, P-JNK, ATF-6 and p-PERK, which was inhibited by Sal B-pretreatment (Fig. 5B).

Pretreatment with Sal B attenuated DOX-induced decrease in myocardial phospho-Akt and phospho-GSK3β

PI3K/Akt is a survival regulation pathway, which can rescues cardiac contractile dysfunction by inhibiting ER stress [39]. PI3K/Akt serves an important function in DOX-induced cardiac dysfunction [40]. The present study also found that DOX decreased phosphorylation of Akt and GSK3β, which can be ameliorated by pretreatment with Sal B (Fig. 6A). To further assess the involvement of PI3K signaling in the cardioprotective effects of Sal B, a selective PI3K antagonist (WM) was used in the next experiment. Sal B-preserved expression in phospho-Akt and phospho-GSK3β was partially abrogated by WM. Also, WM mitigated the inhibition effect of Sal B on GRP78 and CHOP expression. These results suggested that PI3K/Akt may be upstream regulator of ER stress in this pathophysiological process. Sal B may attenuate DOX-induced ER stress partially through PI3K signaling (Fig. 6B). We also evaluated the cardiac function in mice by echocardiography upon stimulation with DOX, Sal B and WM. Data shows that WM decreased EF and FS but increased LVIDs and LVIDd compared with Sal B and DOX co-administrated group (Figs. 7A and 7B).

Discussion

The results of the present study showed that Sal B protected against DOX-induced cardiac dysfunction and cardiomyocyte apoptosis. The salient finding of our study revealed that Sal B significantly inhibited DOX-induced ER stress in mice myocardium, which may be mediated by PI3K/Akt activation.

Several studies have demonstrated that Sal B possesses cardioprotective effects in different models [33]. The present study demonstrated that Sal B significantly increased EF and FS and decreased LVIDs in DOX-treated mice. Sal B also reduced serum levels of AST, LDH and CK in DOX-treated mice. All these results showed that Sal B could prevent DOX-induced cardiac dysfunction and injury. In our preliminary studies, two other methods of Sal B administration were applied, oral administration and intraperitoneal injection. Only pretreatment with Sal B by tail vein injection showed a significant protection against DOX-induced cardiotoxicity

(Supplemental Table S1). The reason for this difference may be attributed to the bad membrane permeation of Sal B.

DOX-induced cardiomyocyte apoptosis has been reported in many studies [41-43] and contributes to the progression of heart failure [44]. TUNEL assay showed that DOX exposure significantly increased DNA fragmentation in the heart of mice, which were inhibited by pretreatment with Sal B. Caspase-3 and Caspase-12 are important in driving the terminal events of apoptosis [45]. Our study showed that DOX increased the protein expression of caspase-3 and caspase-12 in the heart tissues of mice. Moreover, in accordance with previous reports [10, 46], DOX treatment increased pro-apoptotic protein (Bax) expression and decreased anti-apoptotic protein (Bcl-2) expression. However, Sal B could antagonize all these DOX-mediated pro-apoptotic events, suggesting that Sal B protected against DOX-induced cardiotoxicity via inhibiting the apoptosis of cardiomyocyte.

Three different signaling pathways of ER stress transducers have been identified which were mediated by IRE1, ATF6, or PERK. Activated IRE1 interacts with the adaptor protein TRAF2 and initiates a cascade of phosphorylation events that ultimately activates JNK. JNK may induce apoptosis through the pro-apoptotic Bcl-2 family members. Besides, PERK and ATF6 pathways are also involved in the ER stress-associated apoptosis. Activated ATF6 can trigger CHOP, a special pro-apoptosis protein of ER stress. CHOP can down-regulate Bcl-2 and up-regulate BIM. Activation of PERK can also trigger CHOP through phosphorylated eIF2α [47]. Consistent with another study [13], DOX increased the expression of GRP78 and CHOP in cardiac tissues. We also found that ER stress-related apoptosis proteins increased significantly after DOX treatment, including p-IRE-1, p-JNK, ATF-6 and p-PERK. However, pretreatment with Sal B ameliorated these changes, which indicated that Sal B may inhibit DOX-induced apoptosis in mice cardiomyocyte via alleviating ER stress.

PI3K/Akt signaling pathway is involved in many pathophysiological processes and serves an important function in cardiomyocyte survival [17]. Activation of Akt can rescue ER stress-impaired murine cardiac contractile function [20, 39]. Our present study revealed that DOX exposure decreased the phosphorylation of Akt and GSK3β in the heart of mice, which was neutralized by

pre-treatment with Sal B. In order to verify whether PI3K/Akt was involved in Sal B-mediated inhibition of ER stress, mice were pretreated with a selective PI3K antagonist Wortmannin (WM) before DOX administration. The results showed that WM abolished the protection of Sal B against DOX-induced cardiac dysfunction. WM also abrogated the inhibition of Sal B on DOX-induced activation of ER stress-related proteins. These results suggested that Sal B may ameliorate DOX-induced ER stress via activating PI3K/Akt signaling pathway.

Conclusion

In conclusion, our study demonstrated that Sal B attenuated DOX-induced myocardial dysfunction by inhibiting cardiomyocyte apoptosis. The mechanisms may involve the activation of PI3K/Akt signaling pathway and down-regulation of ER stress. These findings demonstrated the potential of Sal B for the treatment of DOX-induced cardiac dysfunction. If the therapeutic roles of Sal B are fully explored in patients and animal models, Sal B treatment can be a promising strategy for reducing the DOX-induced cardiotoxicity in cancer patients.

Acknowledgements

This work was supported by grants (No. 81374011) from the National Natural Sciences Foundation of China and the Major Scientific and Technological Special Project for "Significant New Drugs Formulation" (No. 2012ZX09501001 and No. 2012ZX09301002). The funders had no role in the study design, data collection and analysis, decision to publish or preparation of the manuscript.

Conflict of interest

The authors declared no conflict of interest.

Ethics Statement

All animal experiments were approved by the Medical Ethics Committee of Peking Union Medical College and were in accordance with the national institutes of health regulations for the care and use of animals. All efforts were made to minimize suffering. The acute toxicity study was

carried out according to the up-and-down dosing procedure for testing of chemicals of the Organisation for Economic Cooperation and Development (OECD) guidelines (OECD 2008a).

References

1. S. AlGhamdi, V. Leoncikas, K. E. Plant and N. J. Plant, Synergistic interaction between lipid-loading and doxorubicin exposure in Huh7 hepatoma cells results in enhanced cytotoxicity and cellular oxidative stress: implications for acute and chronic care of obese cancer patients, *Toxicol Res (Camb)*, 2015, **4**, 1479-1487.
2. R. J. Church., J. E. McDuffie., M. Sonee., M. Otieno., J. Y. Ma., X. Liu., P. B. Watkins. and A. H. Harrill., MicroRNA-34c-3p is an early predictive biomarker for doxorubicin-induced glomerular injury progression in male Sprague-Dawley rats, *Toxicol Res (Camb)*, 2014, **3**, 384-394.
3. S. Yamanaka, T. Tatsumi, J. Shiraishi, A. Mano, N. Keira, S. Matoba, J. Asayama, S. Fushiki, H. Fliss and M. Nakagawa, Amlodipine inhibits doxorubicin-induced apoptosis in neonatal rat cardiac myocytes, *Journal of the American College of Cardiology*, 2003, **41**, 870-878.
4. A. Jirkovská-Vávrová., J. Roh., O. Lenčová-Popelová., E. Jirkovský., K. Hrušková., E. Potůčková-Macková., H. Jansová., P. Hašková., P. Martinková., T. Eisner., M. Kratochvíl., J. Šůs., M. Macháček., L. Vostatková-Tichotová., V. Geršl., D. S. Kalinowski., M. T. Muller., D. R. Richardson., K. Vávrová., M. Štěrba and T. Šimůnek., Synthesis and analysis of novel analogues of dexrazoxane and its open-ring hydrolysis product for protection against anthracycline cardiotoxicity in vitro and in vivo, *Toxicol Res (Camb)*, 2015, **4**, 1098-1114
5. R. Arun., S. Dhivya., S. K. Abrahamb. and K. Premkumar., Low-dose chemotherapeutic drugs induce reactive oxygen species and initiate apoptosis-mediated genomic instability, *Toxicol Res (Camb)*, 2016, **5**, 547-556.
6. G. Takemura and H. Fujiwara, Doxorubicin-induced cardiomyopathy from the cardiotoxic mechanisms to management, *Progress in cardiovascular diseases*, 2007, **49**, 330-352.
7. J. Yang, B. Maity, J. Huang, Z. Gao, A. Stewart, R. M. Weiss, M. E. Anderson and R. A. Fisher, G-protein inactivator RGS6 mediates myocardial cell apoptosis and cardiomyopathy caused by doxorubicin, *Cancer research*, 2013, **73**, 1662-1667.
8. J. Ma, Y. Wang, D. Zheng, M. Wei, H. Xu and T. Peng, Rac1 signalling mediates doxorubicin-induced cardiotoxicity through both reactive oxygen species-dependent and -independent pathways, *Cardiovascular research*, 2013, **97**, 77-87.
9. H. Gao, F. Wang, W. Wang, C. A. Makarewich, H. Zhang, H. Kubo, R. M. Berretta, L. A. Barr, J. D. Molkentin and S. R. Houser, Ca(2+) influx through L-type Ca(2+) channels and transient receptor potential channels activates pathological hypertrophy signaling, *Journal of molecular and cellular cardiology*, 2012, **53**, 657-667.
10. H. C. Lai, Y. C. Yeh, L. C. Wang, C. T. Ting, W. L. Lee, H. W. Lee, K. Y. Wang, A. Wu, C. S. Su and T. J. Liu, Propofol ameliorates doxorubicin-induced oxidative stress and cellular apoptosis in rat cardiomyocytes, *Toxicology and applied pharmacology*, 2011, **257**, 437-448.
11. E. J. Ladas, J. S. Jacobson, D. D. Kennedy, K. Teel, A. Fleischauer and K. M. Kelly, Antioxidants and cancer therapy: a systematic review, *Journal of clinical oncology : official journal of the American Society of Clinical Oncology*, 2004, **22**, 517-528.
12. B. J. Sishi, B. Loos, J. van Rooyen and A. M. Engelbrecht, Doxorubicin induces protein

ubiquitination and inhibits proteasome activity during cardiotoxicity, *Toxicology*, 2013, **309**, 23-29.

13. M. Lu, S. Merali, R. Gordon, J. Jiang, Y. Li, J. Mandeli, X. Duan, J. Fallon and J. F. Holland, Prevention of Doxorubicin cardiopathic changes by a benzyl styryl sulfone in mice, *Genes & cancer*, 2011, **2**, 985-992.
14. R. Sano and J. C. Reed, ER stress-induced cell death mechanisms, *Biochimica et biophysica acta*, 2013, DOI: 10.1016/j.bbamcr.2013.06.028.
15. M. Koyama, M. Furuhashi, S. Ishimura, T. Mita, T. Fuseya, Y. Okazaki, H. Yoshida, K. Tsuchihashi and T. Miura, Reduction of endoplasmic reticulum stress by 4-phenylbutyric acid prevents the development of hypoxia-induced pulmonary arterial hypertension, *American journal of physiology. Heart and circulatory physiology*, 2014, DOI: 10.1152/ajpheart.00869.2013.
16. S. Selvaraj, Y. Sun, J. A. Watt, S. Wang, S. Lei, L. Birnbaumer and B. B. Singh, Neurotoxin-induced ER stress in mouse dopaminergic neurons involves downregulation of TRPC1 and inhibition of AKT/mTOR signaling, *The Journal of clinical investigation*, 2012, **122**, 1354-1367.
17. Y. Fujio, T. Nguyen, D. Wencker, R. N. Kitsis and K. Walsh, Akt Promotes Survival of Cardiomyocytes In Vitro and Protects Against Ischemia-Reperfusion Injury in Mouse Heart, *Circulation*, 2000, **101**, 660-667.
18. W. Mao, C. Iwai, J. Liu, S. S. Sheu, M. Fu and C. S. Liang, Darbepoetin alfa exerts a cardioprotective effect in autoimmune cardiomyopathy via reduction of ER stress and activation of the PI3K/Akt and STAT3 pathways, *Journal of molecular and cellular cardiology*, 2008, **45**, 250-260.
19. J. Guo, Y. Bian, R. Bai, H. Li, M. Fu and C. Xiao, Globular adiponectin attenuates myocardial ischemia/reperfusion injury by upregulating endoplasmic reticulum Ca(2)(+)-ATPase activity and inhibiting endoplasmic reticulum stress, *Journal of cardiovascular pharmacology*, 2013, **62**, 143-153.
20. M. Dong, N. Hu, Y. Hua, X. Xu, M. R. Kandadi, R. Guo, S. Jiang, S. Nair, D. Hu and J. Ren, Chronic Akt activation attenuated lipopolysaccharide-induced cardiac dysfunction via Akt/GSK3beta-dependent inhibition of apoptosis and ER stress, *Biochimica et biophysica acta*, 2013, **1832**, 848-863.
21. S. Li, Wan, L., Experimental study on the preventive mechanism of salviae miltiorrhizae against atherosclerosis in rabbits models, *J. Huazhong Univ. Sci.Technol. Med. Sci.*, 2004, **24**, 233-235.
22. L. FF., Y. JH., C. JH. and O. PM., Pharmacological evidence for calcium channel inhibition by Danshen (Salvia miltiorrhiza) on rat isolated femoral artery, *J Cardiovasc Pharmacol*, 2006, **47**, 139-145.
23. Y. Zhou, W. Li, L. Xu and L. Chen, In Salvia miltiorrhiza, phenolic acids possess protective properties against amyloid beta-induced cytotoxicity, and tanshinones act as acetylcholinesterase inhibitors, *Environmental toxicology and pharmacology*, 2011, **31**, 443-452.
24. W. KK., H. MT., L. HQ., L. KF., R. JA., C. RC., F. KP., S. PC. and W. DC., Cryptotanshinone, an acetylcholinesterase inhibitor from Salvia miltiorrhiza, ameliorates scopolamine-induced amnesia in Morris water maze task, *Planta Med*, 2010, **76**, 228-234.
25. H. N. Zhang, C. N. An, H. N. Zhang and X. P. Pu, Protocatechuic acid inhibits neurotoxicity

induced by MPTP in vivo, *Neuroscience letters*, 2010, **474**, 99-103.

26. D. G. Kang, H. Oh, E. J. Sohn, T. Y. Hur, K. C. Lee, K. J. Kim, T. Y. Kim and H. S. Lee, Lithospermic acid B isolated from Salvia miltiorrhiza ameliorates ischemia/reperfusion-induced renal injury in rats, *Life sciences*, 2004, **75**, 1801-1816.
27. W. ZM., W. T., T. YF., L. Y., R. F. and W. H., Effects of salvianolic acid a on oxidative stress and liver injury induced by carbon tetrachloride in rats, *Basic Clin Pharmacol Toxicol*, 2007, **100**, 115-120.
28. H. S. Zhang and S. Q. Wang, Salvianolic acid B from Salvia miltiorrhiza inhibits tumor necrosis factor-alpha (TNF-alpha)-induced MMP-2 upregulation in human aortic smooth muscle cells via suppression of NAD(P)H oxidase-derived reactive oxygen species, *Journal of molecular and cellular cardiology*, 2006, **41**, 138-148.
29. T. XH., X. WJ. and D. XM., Application of Danshen injection on early stage of renal transplantation, *Zhong guo Zhong Xi Yi Jie He Za Zhi*, 2005, **25**, 404-407.
30. S. Chun-Yan., M. Qian-Liang., R. Khalid., H. Ting. and Q. Lu-Ping., Salvia miltiorrhiza: Traditional medicinal uses, chemistry, and pharmacology, *Chinese Journal of Natural Medicines*, 2015, **13**, 0163-0182.
31. L. Xu, Y. Deng, L. Feng, D. Li, X. Chen, C. Ma, X. Liu, J. Yin, M. Yang, F. Teng, W. Wu, S. Guan, B. Jiang and D. Guo, Cardio-protection of salvianolic acid B through inhibition of apoptosis network, *PloS one*, 2011, **6**, e24036.
32. Y. Wang, F. Xu, J. Chen, X. Shen, Y. Deng, L. Xu, J. Yin, H. Chen, F. Teng, X. Liu, W. Wu, B. Jiang and D. A. Guo, Matrix metalloproteinase-9 induces cardiac fibroblast migration, collagen and cytokine secretion: inhibition by salvianolic acid B from Salvia miltiorrhiza, *Phytomedicine : international journal of phytotherapy and phytopharmacology*, 2011, **19**, 13-19.
33. L. Xue, Z. Wu, X.-P. Ji, X.-Q. Gao and Y.-H. Guo, Effect and mechanism of salvianolic acid B on the myocardial ischemia-reperfusion injury in rats, *Asian Pacific Journal of Tropical Medicine*, 2014, **7**, 280-284.
34. M. Wang, G. Sun, P. Wu, R. Chen, F. Yao, M. Qin, Y. Luo, H. Sun, Q. Zhang, X. Dong and X. Sun, Salvianolic Acid B prevents arsenic trioxide-induced cardiotoxicity in vivo and enhances its anticancer activity in vitro, *Evidence-based complementary and alternative medicine : eCAM*, 2013, **2013**, 759483.
35. G. F., S. G., R. X., N. Y., S. J., Q. M. and S. X., Protective effect of salvianolic acid B on isolated heart ischemia/reperfusion injury in rats, *Zhong guo Zhong Yao Za Zhi*, 2012, **37**, 358-361.
36. R. A. Thandavarayan, K. Watanabe, F. R. Sari, M. Ma, A. P. Lakshmanan, V. V. Giridharan, N. Gurusamy, H. Nishida, T. Konishi, S. Zhang, A. J. Muslin, M. Kodama and Y. Aizawa, Modulation of doxorubicin-induced cardiac dysfunction in dominant-negative p38alpha mitogen-activated protein kinase mice, *Free radical biology & medicine*, 2010, **49**, 1422-1431.
37. J. Mersmann, N. Tran, K. Latsch, K. Habeck, F. Iskandar, R. Zimmermann and K. Zacharowski, Akt or phosphoinositide-3-kinase inhibition reverses cardio-protection in Toll-like receptor 2 deficient mice, *Resuscitation*, 2012, **83**, 1404-1410.
38. K. Drosatos, Z. Drosatos-Tampakaki, R. Khan, S. Homma, P. C. Schulze, V. I. Zannis and I. J. Goldberg, Inhibition of c-Jun-N-terminal kinase increases cardiac peroxisome proliferator-activated receptor alpha expression and fatty acid oxidation and prevents lipopolysaccharide-induced heart dysfunction, *The Journal of biological chemistry*, 2011, **286**, 36331-36339.

39. Y. Zhang, Z. Xia, K. H. La Cour and J. Ren, Activation of Akt rescues endoplasmic reticulum stress-impaired murine cardiac contractile function via glycogen synthase kinase-3beta-mediated suppression of mitochondrial permeation pore opening, *Antioxidants & redox signaling*, 2011, **15**, 2407-2424.

40. G. C. Fan, X. Zhou, X. Wang, G. Song, J. Qian, P. Nicolaou, G. Chen, X. Ren and E. G. Kranias, Heat shock protein 20 interacting with phosphorylated Akt reduces doxorubicin-triggered oxidative stress and cardiotoxicity, *Circulation research*, 2008, **103**, 1270-1279.

41. S. Kotamraju, E. A. Konorev, J. Joseph and B. Kalyanaraman, Doxorubicin-induced apoptosis in endothelial cells and cardiomyocytes is ameliorated by nitrone spin traps and ebselen. Role of reactive oxygen and nitrogen species, *The Journal of biological chemistry*, 2000, **275**, 33585-33592.

42. I. Andreadou, F. Sigala, E. K. Iliodromitis, M. Papaefthimiou, C. Sigalas, N. Aligiannis, P. Savvari, V. Gorgoulis, E. Papalabros and D. T. Kremastinos, Acute doxorubicin cardiotoxicity is successfully treated with the phytochemical oleuropein through suppression of oxidative and nitrosative stress, *Journal of molecular and cellular cardiology*, 2007, **42**, 549-558.

43. L. E. Wold, N. S. Aberle, 2nd and J. Ren, Doxorubicin induces cardiomyocyte dysfunction via a p38 MAP kinase-dependent oxidative stress mechanism, *Cancer detection and prevention*, 2005, **29**, 294-299.

44. D. B. Sawyer, R. Fukazawa, M. A. Arstall and R. A. Kelly, Daunorubicin-Induced Apoptosis in Rat Cardiac Myocytes Is Inhibited by Dexrazoxane, *Circulation Research*, 1999, **84**, 257-265.

45. K. N. Kim, Y. M. Ham, J. Y. Moon, M. J. Kim, Y. H. Jung, Y. J. Jeon, N. H. Lee, N. Kang, H. M. Yang, D. Kim and C. G. Hyun, Acanthoic acid induces cell apoptosis through activation of the p38 MAPK pathway in HL-60 human promyelocytic leukaemia, *Food chemistry*, 2012, **135**, 2112-2117.

46. L. Fujimura, Y. Matsudo, M. Kang, Y. Takamori, T. Tokuhisa and M. Hatano, Protective role of Nd1 in doxorubicin-induced cardiotoxicity, *Cardiovascular research*, 2004, **64**, 315-321.

47. D. Ron and P. Walter, Signal integration in the endoplasmic reticulum unfolded protein response, *Nature reviews. Molecular cell biology*, 2007, **8**, 519-529.

435

436 **Figure legends**

437 **Fig. 1.** Effects of Sal B and DOX on body weight. (A) Molecular structure of Sal B. (B) Body weights and heart
438 weights (C) of mice were measured 7 d after DOX injection. (D) Relative heart weight index (heart
439 weight-to-body weight ratio) was determined. Data are presented as mean ± SE, *P < 0.05 vs. Cont group; #P
440 <0.05 vs. DOX group.

441 **Fig. 2.** Effects of Sal B and DOX on cardiac function. (A) Representative M-mode echocardiography images are
442 shown. (B) Echocardiography values are expressed as mean ± SE. EF, ejection fraction; FS, fractional shortening;
443 LVIDd, left ventricular internal diameter at diastolic phase; LVIDs, left ventricular internal diameter at systolic
444 phase. Data are presented as mean ± SE, *P < 0.05 vs. Cont group; #P <0.05 vs. DOX group.

445 **Fig. 3.** Effects of Sal B on DOX-induced myocardial injury. (A) Effects of Sal B and DOX on AST, LDH and CK
446 activities. (B) Effects of Sal B and DOX on histological changes in mice hearts by HE staining (scale bar = 10 μm).
447 (C) Effects of Sal B and DOX on ultrastructure changes in mice hearts observed under electron microscope (scale
448 bar = 200 pm). (D) Effects of Sal B and DOX on the mice ECG pattern. (E) Effects of Sal B and DOX on the heart
449 rate of mice. Data are presented as mean ± SE, *P < 0.05 vs. Cont group; #P <0.05 vs. DOX group.

450 **Fig. 4.** Effects of Sal B and DOX on heart apoptosis and apoptosis related proteins. (A) Representative images of
451 TUNEL and DAPI staining of myocardium tissue and quantification of TUNEL-positive cells (scale bar = 10 μm).
452 Arrowheads in the pictures indicate the nuclei of apoptotic cells; blue color represents cell nuclei that were
453 counterstained with DAPI. (B) Effects of Sal B and DOX on protein expression of cleaved caspase-3, caspase-3,
454 cleaved caspase-12 and caspase-12. (C) Effects of Sal B and DOX on protein expression of Bcl-2 and Bax. Data
455 are presented as mean ± SE, *P < 0.05 vs. Cont group; #P <0.05 vs. DOX group.

456 **Fig. 5.** Effects of Sal B and DOX on ER stress sensors and ER stress-related apoptotic protein expression in heart
457 tissues. (A) Western blot analysis of GRP78 and CHOP. (B) Western blot analysis of p-IRE1, IRE-1, p-JNK, JNK,
458 ATF-6, p-PERK and PERK. Data are presented as mean ± SE, *P < 0.05 vs. Cont group; #P <0.05 vs. DOX group.

459 **Fig. 6.** Effects of Sal B and DOX on protein expression of PI3K/Akt signaling pathway. (A) Protein levels of
460 p-AKT, AKT, p-GSK3β and GSK3β in the myocardium examined by Western blot analysis. (B) Effects of

pharmacological inhibitor WM (a selective PI3K antagonist) on levels of p-AKT, p-GSK3β, GRP78, CHOP, in the myocardium of Sal B and DOX co-treated mice. Data are presented as mean ± SE, *P < 0.05 vs. Cont; #P < 0.05 vs. DOX-treated mice; $P <0.05 vs. Sal B and DOX co-treated mice.

Fig. 7. Involvement of PI3K/Akt signaling in DOX-induced cardiac dysfunction. (A) Cardiac function was examined by echocardiography 7 d after DOX administration. Representative M-mode echocardiography images are shown. (B) Echocardiography values are expressed as mean ± SE. EF, ejection fraction; FS, fractional shortening; LVIDd, left ventricular internal diameter at diastolic phase; LVIDs, left ventricular internal diameter at systolic phase. Data are presented as mean ± SE, *P < 0.05 vs. Cont; #P < 0.05 vs. DOX-treated mice; $P <0.05 vs. Sal B and DOX co-treated mice.

Fig. 1.

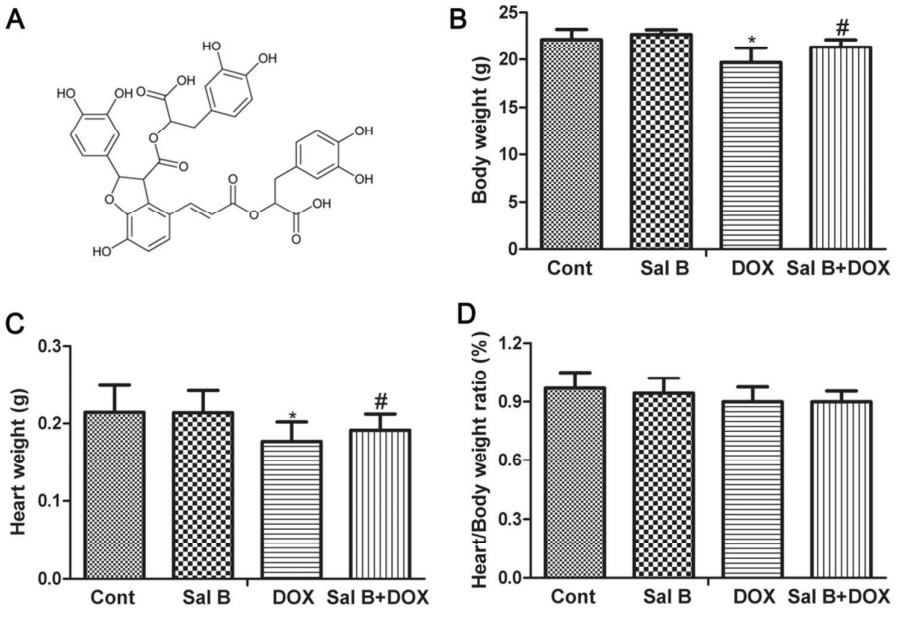

Fig. 2.

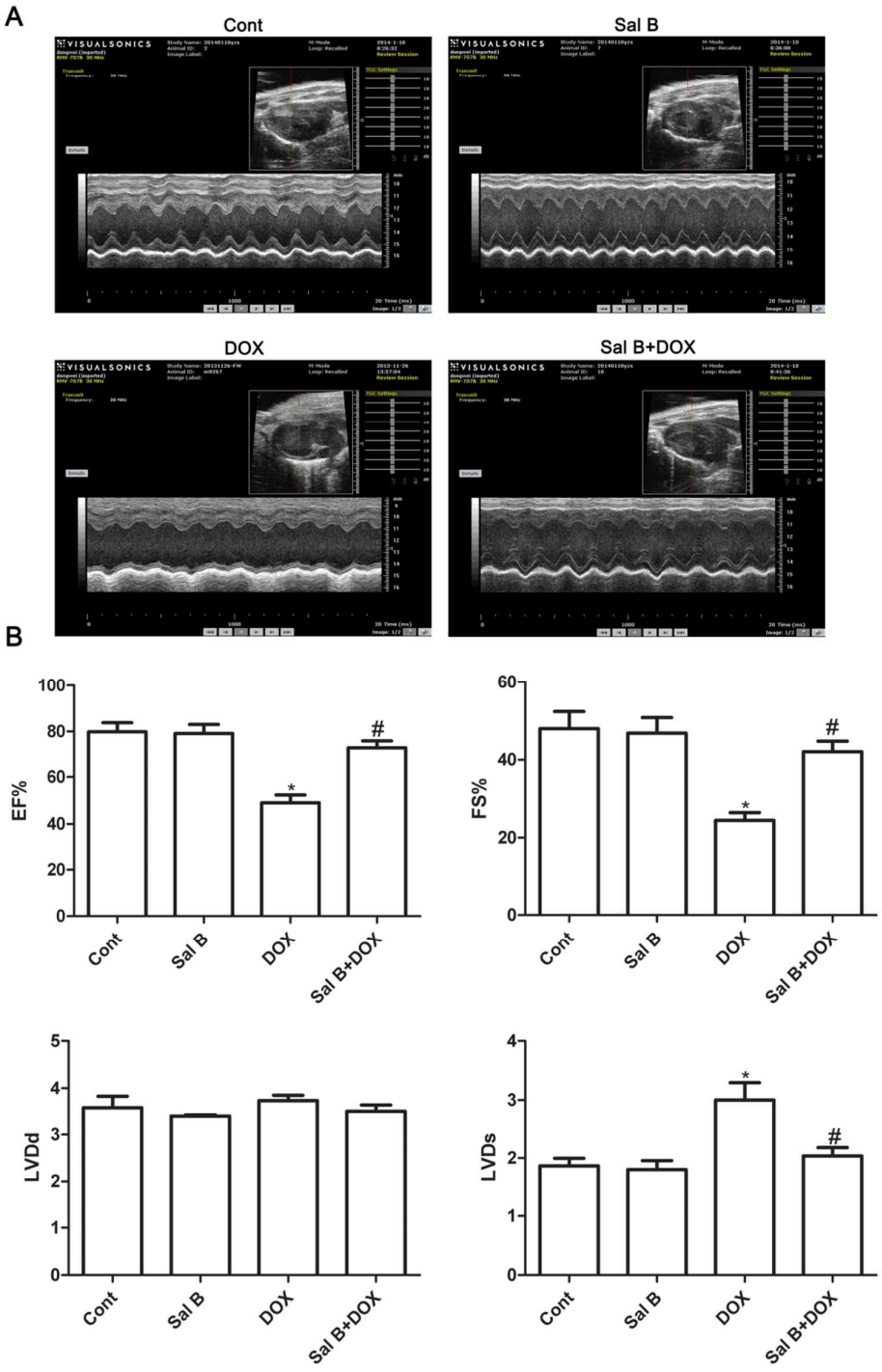

Fig. 3.

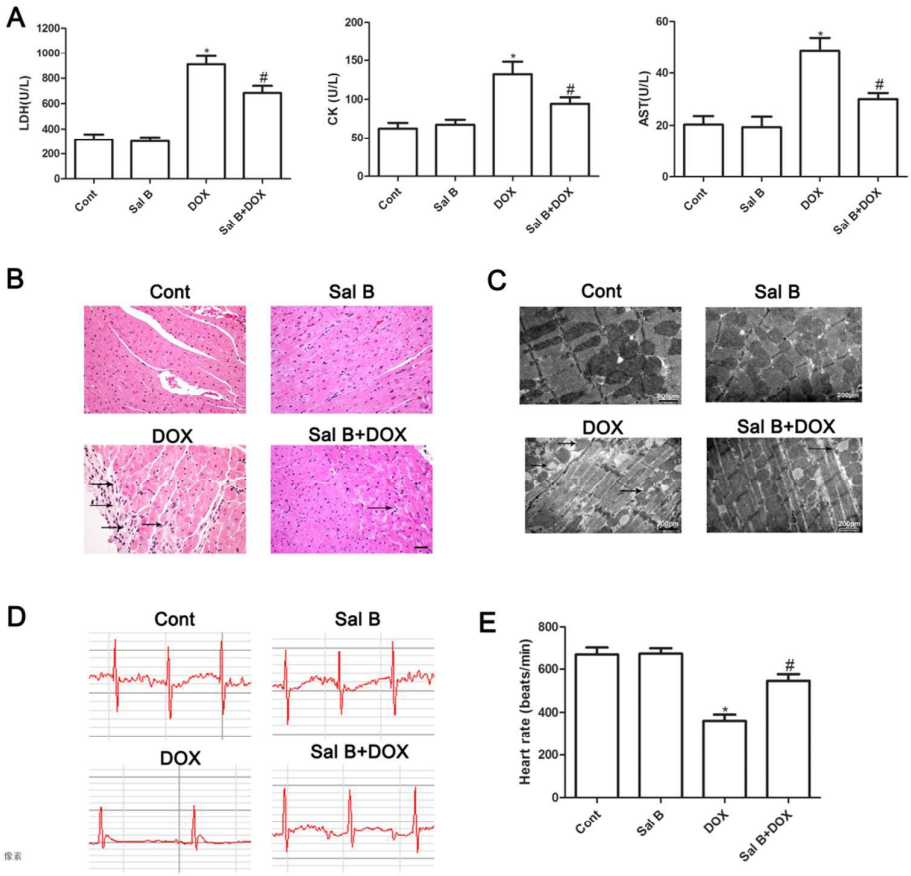

492 **Fig. 4.**

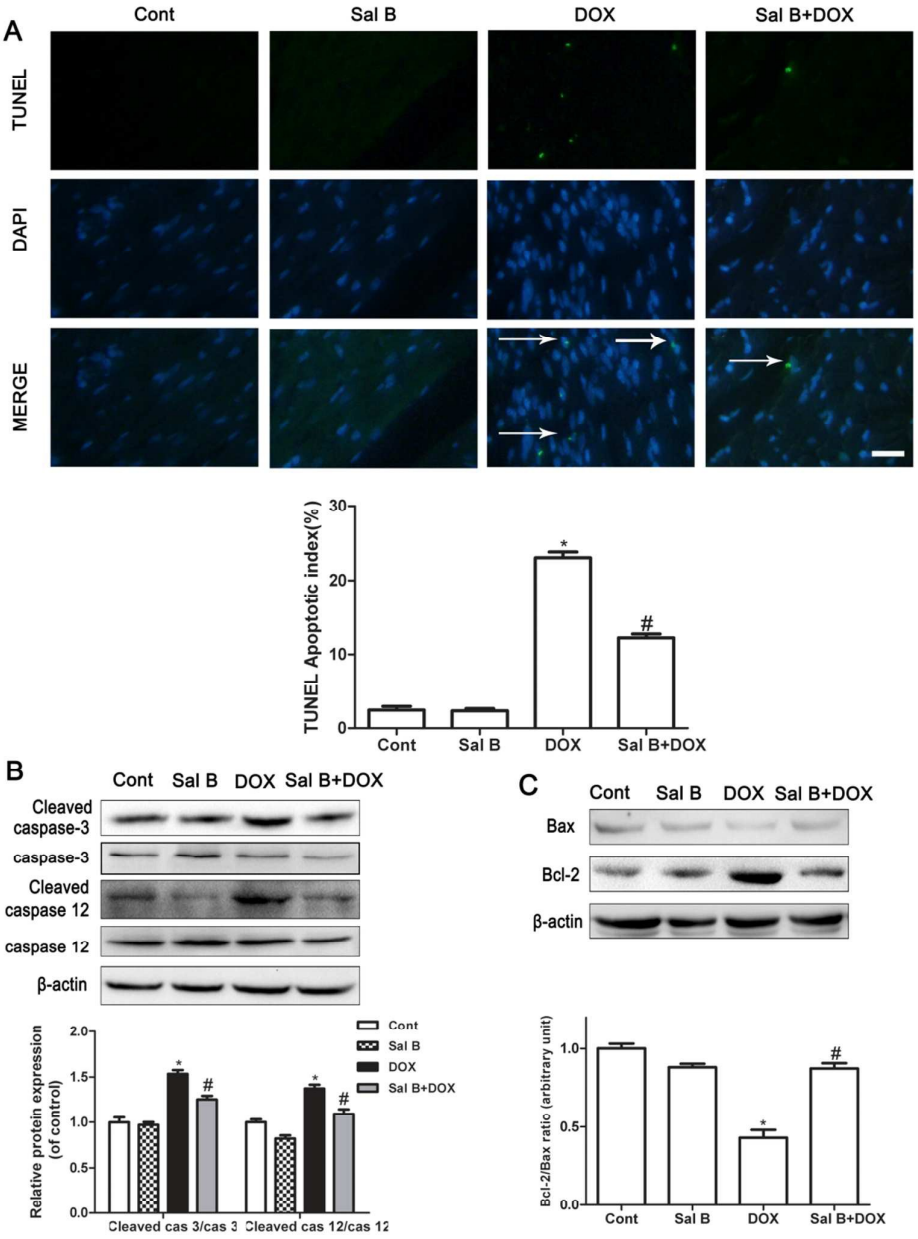

493

494

495

496

Fig. 5.

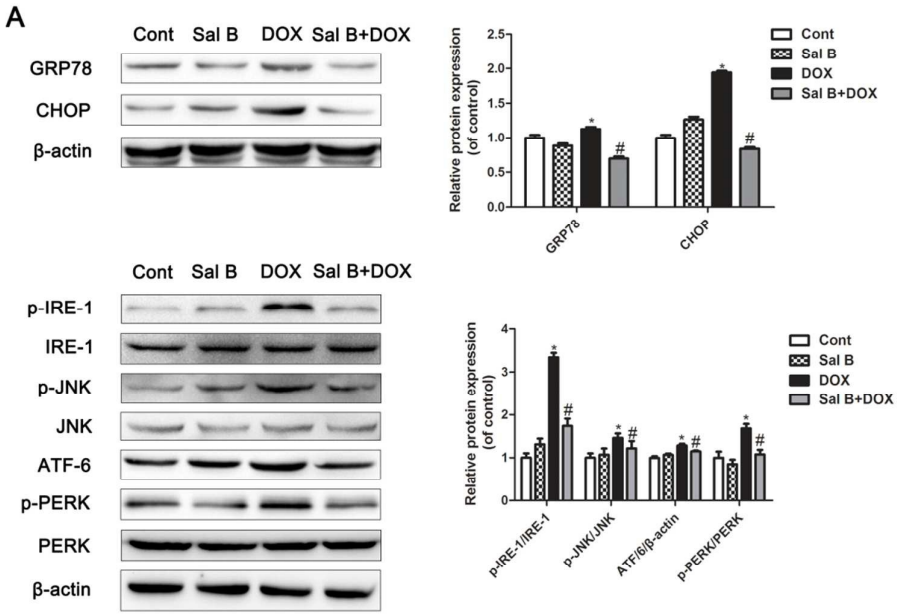

Fig. 6.

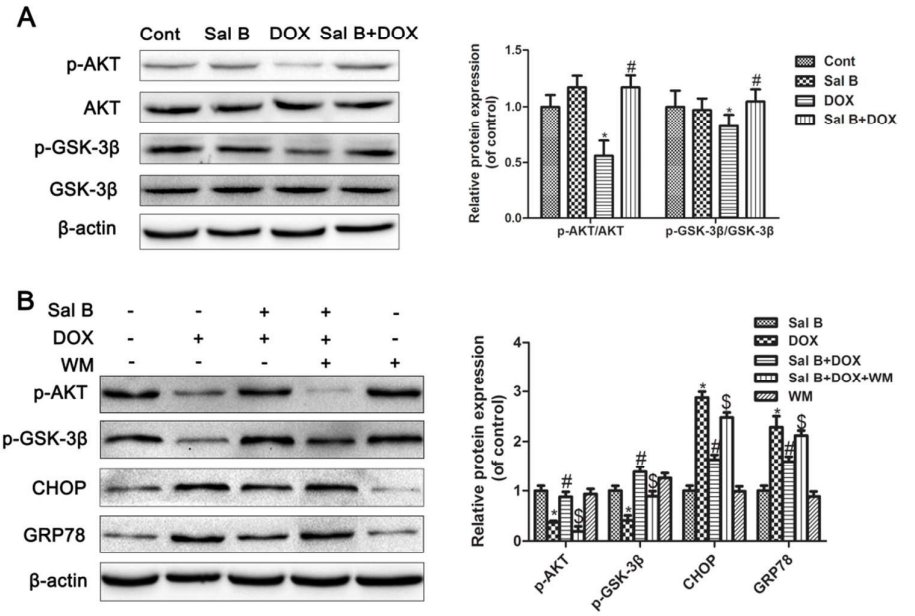

Fig. 7.

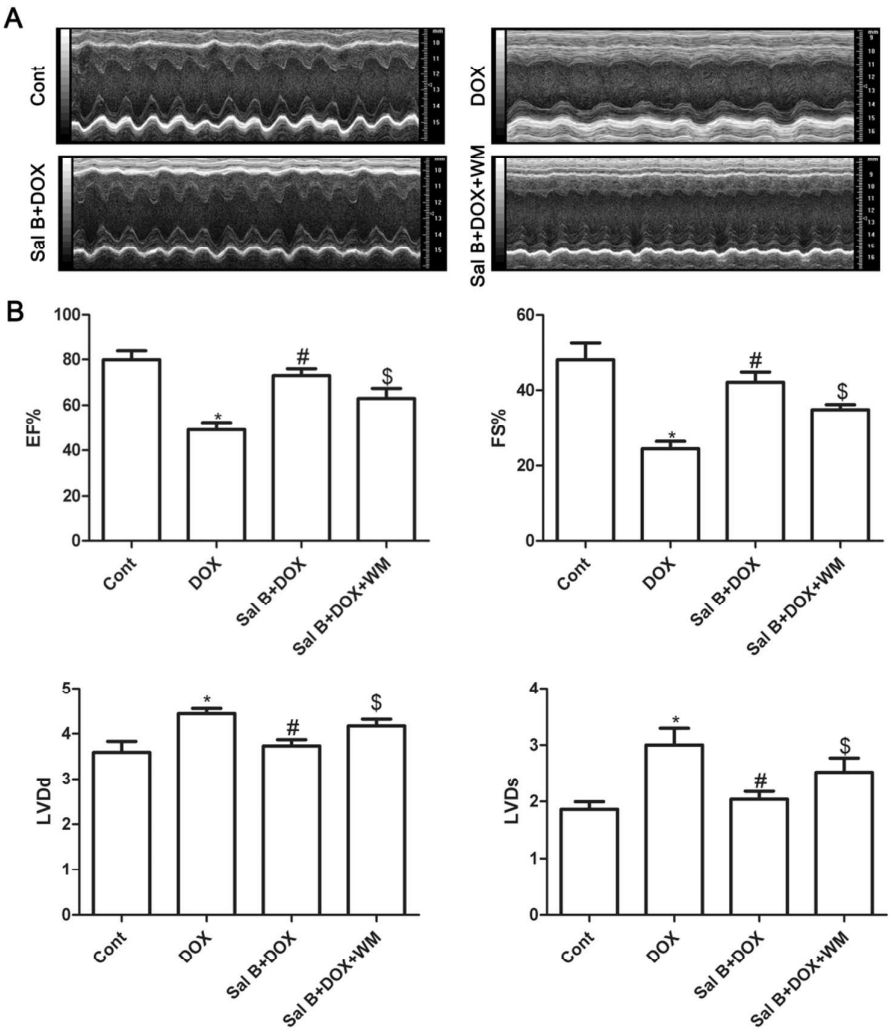

504

Salvianolic acid B protects against doxorubicin-induced cardiac dysfunction via inhibition of ER-stress-mediated cardiomyocyte apoptosis